Smart Structures and Systems, *Vol. 19, No. 1 (2017) 11-20*
DOI: https://doi.org/10.12989/sss.2017.19.1.011

Damage detection of shear buildings through structural mass-stiffness distribution

Yabin Liang[1,2], Dongsheng Li[*1], Gangbing Song[1,2] and Chao Zhan[1]

[1]*Faculty of Infrastructure Engineering, Dalian University of Technology, Dalian, Liaoning, China*
[2]*Department of Mechanical Engineering, University of Houston, Houston, TX, USA*

(Received December 16, 2015, Revised September 14, 2016, Accepted September 16, 2016)

Abstract. For structural damage detection of shear buildings, this paper proposes a new concept using structural element mass-stiffness vector (SEMV) based on special mass and stiffness distribution characteristics. A corresponding damage identification method is developed combining the SEMV with the cross-model cross-mode (CMCM) model updating algorithm. For a shear building, a model is assumed at the beginning based on the building's distribution characteristics. The model is updated into two models corresponding to the healthy and damaged conditions, respectively, using the CMCM method according to the modal parameters of actual structure identified from the measured acceleration signals. Subsequently, the structural SEMV for each condition can be calculated from the updated model using the corresponding stiffness and mass correction factors, and then is utilized to form a new feature vector in which each element is calculated by dividing one element of SEMV in health condition by the corresponding element of SEMV in damage condition. Thus this vector can be viewed as a damage detection feature for its ability to identify the mass or stiffness variation between the healthy and damaged conditions. Finally, a numerical simulation and the laboratory experimental data from a test-bed structure at the Los Alamos National Laboratory were analyzed to verify the effectiveness and reliability of the proposed method. Both simulated and experimental results show that the proposed approach is able to detect the presence of structural mass and stiffness variation and to quantify the level of such changes.

Keywords: structural element mass-stiffness vector; damage identification; cross-model cross-mode method; shear building

1. Introduction

Many civil infrastructure, especially high-rise buildings and long-span bridges built after World War II, are facing the problem of deterioration and need measures to evaluate their safety. With recent advances of sensing techniques, structural health monitoring (SHM) are thus emerging as an enabling mean to monitor the operational performance and health conditions of important civil structures, newly built or old ones (Li, Li *et al.* 2004, Farrar and Worden 2012). Among many evaluation techniques, vibration-based damage detection is a promising field in SHM (Doebling, Farrar *et al.* 1998, Fan and Qiao 2011). The basic principle is that damage changes structural properties and structural damage can thus be inversely determined through the monitoring of those changes of structural properties. Such structural property changes, usually termed as damage feature in the field of damage identification or SHM, can be alterations of structural natural frequencies, mode shapes, modal damping, mode strain energy, and frequency response functions, etc. Many vibration-based damage detection methods have been proposed and interested readers may consult excellent references (Sohn, Farrar *et al.* 2004, Carden and Fanning 2004). In general, these methods can be characterized by the fact that whether a theoretical analytical model is involved or not as model-based methods and non-model based methods. For model-based damage detection methods, changes of structure parameters are identified by comparing actual measured data with corresponding ones calculated from a theoretical model. A significant advantage of model-based methods is their ability to identify damage location and extent simultaneously. Wang (2009) extended cross-model cross-mode (CMCM) model updating method proposed by Hu, Li *et al.* (2007) to damage detection area. Excellent damage detection results were shown for a benchmark model and an offshore jacket platform structure when theoretical models were precisely established and test modal information were identified accurately. However, it is, in many cases, difficult or even impossible to establish a precise theoretical model for an actual structure, which hinders wide application of model-based damage detection methods. On the other hand, non-model based damage detection techniques are gaining popularity among researchers since these techniques do not need theoretical models and are more practical for existing structures than model-based approaches. Among the non-model based detection methods, those based on modal parameters are widely used since modal parameters are inherent characteristics of a structure and will not change with external excitation levels. Pandey, Biswas *et al.* (1991) proposed mode shape curvature as a sensitive parameter for

[*]Corresponding author, Ph.D.
E-mail: dsli@dlut.edu.cn

ISSN: 1738-1584 (Print), 1738-1991 (Online)

damage localization. Mode shape curvature was calculated using the central difference approximation and then utilized for damage localization of a simulated beam discretized into a number of finite elements. Sampaio, Maia *et al.* (1999) extended the idea of Pandey, Biswas *et al.* (1991) by applying the curvature-based method to frequency response function and demonstrated the potential of their approach with actually measured data. Tomaszewska (2010) applied a flexibility-based approach and a mode shape curvature-based approach on a simulated beam and a real historical tower building to study the effect of statistical errors. Zhu, Li *et al.* (2011) demonstrated the efficacy of the change in the slope of the fundamental mode shape as a damage indication feature by performing a numerical study on an eight-story shear building and conducting experiments on a three-story building model. An iterative scheme was developed to locate structural damage and the magnitude of damage was quantified using the proposed mode shape slope-based feature. Also, a mathematical basis was provided by Roy and Ray-Chaudhuri (2013) to show the correlation between structural damage and a change in the fundamental mode shape, as well as its derivatives, such as shape slope, shape curvature and flexibility. Many of these methods require certain transformations of measured data to get a more sensitive feature for damage identification. As is well known, data transformations or derivative computation are more sensitive to noise contamination. Moreover, many methods still remain at the level of damage presence or location detection.

In order to overcome these disadvantages, some innovative approaches have been proposed by researchers. Among them, the restoring force method proposed by Masri, Bekey *et al.* (1982) is one verified and feasible damage identification approach for shear buildings (Masri, Bekey *et al.* 1982, Worden and Tomlinson 1989, Hernandez-Garcia, Masri *et al.* 2010). Based on the restoring force method, Hernandez-Garcia, Masri *et al.* (2010) proposed a data-driven non-parametric identification technique for uncertain MDOF chain-like systems, in which the variation value of corresponding restoring force coefficients between health and test conditions was regarded as a damage detection feature. The technique could detect the presence of structural changes, locate the structural section where changes occur, and provide an accurate estimate of actual level of “changes”. However, the floor mass ratios in this approach are required to be presumed in advance. Moreover, how to reconstruct the relative displacements and velocities between neighboring floors is also debatable.

In this paper, a concept of structural element mass-stiffness vector (SEMV) is introduced and a new data-driven non-parametric identification technique is proposed for structural change detection. The proposed damage detection approach combines the SEMV with the cross-model cross-mode (CMCM) model updating method and thus has the advantages of model-based and output-only non-parametric based damage identification methods mentioned above : (1) no physical parameters of actual structure are needed but a few of structural modes identified from the measured acceleration signals in health and damage conditions; (2) not only structural element stiffness decrease but also element mass change can be identified. (3) both damage location and extent can be accurately detected and evaluated.

In what follows, the CMCM method and the concept of SEMV are introduced briefly. Then the theoretical formulation of the proposed method is presented followed with a numerical simulation example. Finally, experimental data from a test-bed structure tested at the Los Alamos National Laboratory are employed to validate the proposed approach. Both the simulation and experiment results show that the proposed method could detect the presence of structural damage, locate damage and determine damage severity.

2. Fundamentals of cross-model cross-mode method

Cross-model cross-mode (CMCM) method was originally developed by Hu, Li *et al.* (2007) as one physical property adjustment approach for model updating, and was later generalized to damage detection. An attractive feature of the CMCM method is that it requires only a few measured modes of the damaged structure and the measured modes do not require to pair or scale (mass-normalize) with the analytical modes. In this section, the theoretical background and rationale of the CMCM method are presented. The material is well known and expounded here repeatedly for the sake of clarity and the derivation of our improvement in section three.

In the CMCM method, it is assumed that the stiffness and mass matrices of a structure, denoted by **K** and **M**, respectively, are already obtained from a finite-element model. The stiffness matrix $\mathbf{K}^*$ and mass matrix $\mathbf{M}^*$ of the experimental model are assumed to be a modification of **K** and **M** of the theoretical model and can be formulated as

$$\begin{cases} \mathbf{K}^* = \mathbf{K} + \sum_{n=1}^{Ne} \alpha_n \mathbf{K}_n^e \\ \mathbf{M}^* = \mathbf{M} + \sum_{n=1}^{Ne} \beta_n \mathbf{M}_n^e \end{cases} \tag{1}$$

where $\mathbf{K}_n{}^e$, $\mathbf{M}_n{}^e$ are the stiffness and mass matrix corresponding to the *n*th element; N_e is number of elements; α_n and β_n are the *n*th element stiffness and mass correction factors to be determined, respectively. In the CMCM method, It is intended to ‘‘correct’’ or ‘‘update’’ the stiffness and mass matrices by modal measurements, including a few mode shapes and corresponding frequencies. So the structural updating equation using the CMCM method can be expressed as

$$\sum_{n=1}^{Ne} \alpha_n C_{n,ij} + \sum_{n=1}^{Ne} \beta_n E_{n,ij} = f_{ij} \tag{2}$$

where

$$\begin{cases} C_{n,ij} = \left(\Phi_i\right)^T \mathbf{K}_n^e \Phi_j^* \\ E_{n,ij} = -\lambda_j^* \left(\Phi_i\right)^T \mathbf{M}_n^e \Phi_j^* \\ f_{ij} = \lambda_j^* \left(\Phi_i\right)^T \mathbf{M} \Phi_j^* - \left(\Phi_i\right)^T \mathbf{K} \Phi_j^* \end{cases} \tag{3}$$

where $\mathbf{\Phi}_i$ means the ith eigenvector of initial finite-element model, Φ_j^* and λ_j^* denote the jth eigenvector and eigenvalue of the to-be-updated structure, respectively. When N_i reliable modes are available from the finite-element model, and N_j modes are measured from the corresponding real structure, totally $N_m=N_i\times N_j$ CMCM equations can be formed in Eq. (2). Using a new index m to replace ij, Eq. (2) becomes

$$\sum_{n=1}^{Ne}\alpha_n C_{n,m}+\sum_{n=1}^{Ne}\beta_n E_{n,m}=f_m \tag{4}$$

written in a matrix form, one has

$$\mathbf{G\gamma}=\mathbf{f} \tag{5}$$

where $\mathbf{G}$ = [$\mathbf{C}$ $\mathbf{E}$], $\boldsymbol{\gamma}$ = [$\boldsymbol{\alpha}$, $\boldsymbol{\beta}$]^T, in which $\mathbf{C}$ and $\mathbf{E}$ are $N_m\times N_e$ matrix; $\boldsymbol{\alpha}$ and $\boldsymbol{\beta}$ are column vector of size N_e; and $\mathbf{f}$ is a column vector of size N_m. If N_m is greater than $2N_e$—more equations are available than unknowns, one would expect that a least-squares solution for $\boldsymbol{\gamma}$ can be taken.

One feature associated with the formulation of Eq. (1) is that all the non-zero coefficients of $\mathbf{M}^*$ and $\mathbf{K}^*$ are allowed to change upon varying the correction factors $\boldsymbol{\alpha}$ and $\boldsymbol{\beta}$. This particular situation can be termed as a complete-updating case, in contrast to a partial-updating case that one or more non-zero coefficients of $\mathbf{M}^*$ and $\mathbf{K}^*$are not allowed to vary (Wang 2009). If the updated matrices $\mathbf{M}^*$ and $\mathbf{K}^*$ in Eq. (1) are replaced by $a\mathbf{M}^*$ and $a\mathbf{K}^*$ where a is an arbitrary positive constant not equal to 1, it would correspond to a different set of correction factors. While these two dynamic systems, characterized by ($\mathbf{M}^*$, $\mathbf{K}^*$) and ($a\mathbf{M}^*$, $a\mathbf{K}^*$), respectively, are different in spatial domain, they are identical in the modal space, i.e., they possess the same eigenvalues λ_j^* and $\mathbf{\Phi}_j^*$. Since the CMCM equations in Eq. (2) are derived based on the usage of λ_j^* and $\mathbf{\Phi}_j^*$, the corresponding solutions for the correction factors should apply to both dynamic systems. From the above observations, one concludes that multiple sets of solutions for the correction factors exist for a complete-updating case. In theory, to gain a unique solution for the correction factors, at least an additional constraint equation must be imposed. For instance, a particular mass or stiffness element is predetermined, or the total mass of the system is known, etc.

3. Damage identification for shear buildings

3.1 Typical characteristics of shear buildings

A typical shear building is shown in Fig. 1. Denote the lateral stiffness of the ith story by k_i, the element stiffness matrix of the ith element that connects the (i-1)th and ith floor is given as $\mathbf{k}_i^e$, Then the system stiffness matrix $\mathbf{K}$ for the n-story shear building can be assembled as

$$\mathbf{K}=\sum_{i=1}^{n}\mathbf{K}_i^e=\begin{bmatrix} k_1+k_2 & -k_2 & 0 & \cdots & 0 \\ -k_2 & k_2+k_3 & -k_3 & 0 & \vdots \\ 0 & -k_3 & \ddots & 0 & 0 \\ \vdots & 0 & 0 & k_{n-1}+k_n & -k_n \\ 0 & \cdots & 0 & -k_n & k_n \end{bmatrix} \tag{6}$$

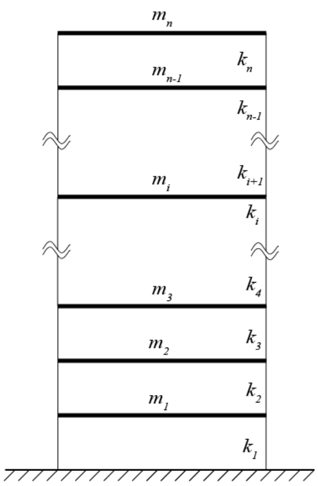

Fig. 1 Diagram of an n-story shear building

where $\mathbf{K}_i^e$ denotes the corresponding element stiffness matrix $\mathbf{k}_i^e$ in the global coordinates. Let the mass of the ith floor be m_i, the corresponding system mass matrix $\mathbf{M}$ is written as $\mathbf{M}=\sum_{i=1}^{n}\mathbf{M}_i^e$= diag($m_1$, m_2, ⋯, m_{n-1}, m_n), where $\mathbf{M}_i^e$ denotes the corresponding m_i in the global coordinates.

The eigenvalue λ and eigenvector $\mathbf{\Phi}$ could be computed by eigenvalue decomposition of structure mass matrix $\mathbf{M}$ and stiffness matrix $\mathbf{K}$, which are established by the mass vector $\mathbf{m}$ = [m_1, m_2, ⋯, m_n] and stiffness vector $\mathbf{k}$ = [k_1, k_2, ⋯, k_n] in the way mentioned above.

3.2 Structural element mass-stiffness vector for shear buildings

According to section two, only one constraint is required to realize complete model updating for all the mass and stiffness parameters using the CMCM method for shear buildings. It is assumed here that m_1 is known as the necessary constraint. The mass and stiffness vectors can thus be written as

$$\begin{cases}\bar{\mathbf{m}}=\left[m_1,\hat{m}_2,\hat{m}_3,\cdots,\hat{m}_n\right]\\ \bar{\mathbf{k}}=\left[\hat{k}_1,\hat{k}_2,\hat{k}_3,\cdots,\hat{k}_n\right]\end{cases} \tag{7}$$

where $\hat{m}_i,\hat{k}_i$ (i=1,2,⋯,n) denote the mass and stiffness values of the initial to-be-updated model, respectively.

If this to-be-updated model exists, all the structural parameters, including corresponding mass matrix $\hat{\mathbf{M}}$, stiffness matrix $\hat{\mathbf{K}}$, element mass and stiffness matrix $\hat{\mathbf{M}}_i^e$, $\hat{\mathbf{K}}_i^e$ (i=1,2,⋯,n) denoted in the global coordinates, eigenvalue $\hat{\lambda}$ and eigenvector $\hat{\mathbf{\Phi}}$ of the given to-be-updated model, could be obtained as shown in section 3.1. Consequently, all the stiffness and mass correction factors $\hat{\boldsymbol{\alpha}}$, $\hat{\boldsymbol{\beta}}$ of the to-be-updated model could be calculated.

The updated mass and stiffness of the model can be given by

$$\begin{cases}m_1=m_1\\ m_i=\hat{m}_1(1+\hat{\beta}_i)\ \ (i=2,3,\cdots,n)\\ k_i=\hat{k}_1(1+\hat{\alpha}_i)\ \ (i=1,2,3,\cdots,n)\end{cases} \tag{8}$$

where m_i and k_i denote the updated element mass and stiffness, respectively, which equal to actual structural physical parameters. Thus, a conclusion could be drawn from above theoretical analysis: although given initial models may differ in their spatial and modal properties ($\widehat{\mathbf{K}}$, $\widehat{\mathbf{M}}$, $\widehat{\mathbf{K}}_{it}$, $\widehat{\mathbf{M}}_{it}$, $\widehat{\boldsymbol{\Phi}}$, $\widehat{\lambda}$), corresponding stiffness and mass correction factors $\widehat{\boldsymbol{\alpha}}$, $\widehat{\boldsymbol{\beta}}$, the final updated model is the same ($\mathbf{K}$, $\mathbf{M}$, $\mathbf{K}_{nt}$, $\mathbf{M}_{nt}$, $\boldsymbol{\Phi}$, λ) which must agree with actual modal measurements, i.e. no matter what the initial given model is, the physical parameters of an actual structure could be obtained after model updating according to Eq. (8). Therefore, the final updated model is less susceptible to the assumed values of initial $\widehat{m}_i$,$\widehat{k}_i$ and the given model could finally be corrected or updated to true structural element mass and stiffness using the CMCM method.

According to the above analysis, a convenient approach is adopted in the work. If all the element mass and stiffness of a given to-be-updated model equal to m_1 (denoted by $\widehat{m}_i = m_1$,$\widehat{k}_i = m_1$), then the updated mass and stiffness, denoted as the vector form $\mathbf{Z}=[m_1, m_2,\cdots, m_n, k_1, k_2,\cdots, k_n]$, can be written as

$$\mathbf{Z} = m_1 \mathbf{V}_{m1} \tag{9}$$

where

$$\mathbf{V}_{m1} = \left[1, \left(1+\bar{\beta}_2\right), \left(1+\bar{\beta}_3\right), \cdots, \left(1+\bar{\beta}_n\right), \left(1+\bar{\alpha}_1\right), \left(1+\bar{\alpha}_2\right), \cdots, \left(1+\bar{\alpha}_n\right)\right] \tag{10}$$

The vector $\mathbf{V}_{m1}$ can also be interpreted as the normalization of vector $\mathbf{Z}$ at the location of m_1, i.e. $1+\bar{\beta}_i=m_i/m_1$,$1+\bar{\alpha}_j=k_j/m_1$ (i=2,3,$\cdots$,n , j=1,2,3,$\cdots$,n). At the same time, It is worth noting that the calculation of the vector $\mathbf{V}_{m1}$ is based on the assumption that m_1 has been predetermined, however, the final value of $\mathbf{V}_{m1}$has nothing to do with m_1 since $\mathbf{V}_{m1}$is normalized at that location. The vector $\mathbf{V}_{m1}$ in Eq. (10) can be termed as m_1-normalized structural element mass-stiffness vector (SEMV). The SEMV vector $\mathbf{V}_{m1}$, which represents the mass and stiffness distribution in certain sequence, is the inherent property of an actual structure and can be used for damage detection.

If only the SEMV $\mathbf{V}_{m1}$ is concerned, m_1 can be any positive constant for a given to-be-updated model in which $\widehat{m}_i = m_1$, $\widehat{k}_i = m_1$ according to the procedures mentioned above. A SEMV is then obtained by substituting the correction factors $\overline{\boldsymbol{\alpha}}, \overline{\boldsymbol{\beta}}$ of the to-be-updated model into Eq. (10) with the CMCM method. Likewise, if it is assumed that another parameter has been predetermined (such as k_1), the same is true for all the previous theoretical analysis and conclusion. The only difference is that the element value corresponding to k_1 changes to 1 in the k_1-normalized SEMV.

3.3 Damage identification using SEMV

As analyzed in section 3.2, a SEMV represents the inherent mass and stiffness distribution property of a structure and can thus be used for structural damage detection. Assume that the SEMV of a structure in health condition is expressed as

$$\mathbf{V}_{\mathrm{H},m1} = \left[1, \frac{m_2}{m_1}, \frac{m_3}{m_1}, \cdots, \frac{m_n}{m_1}, \frac{k_1}{m_1}, \frac{k_2}{m_1}, \cdots, \frac{k_n}{m_1}\right] \tag{11}$$

Likewise, the SEMV of a structure in damage condition is

$$\mathbf{V}_{\mathrm{D},m1} = \left[1, \frac{m_2^*}{m_1^*}, \frac{m_3^*}{m_1^*}, \cdots, \frac{m_n^*}{m_1^*}, \frac{k_1^*}{m_1^*}, \frac{k_2^*}{m_1^*}, \cdots, \frac{k_n^*}{m_1^*}\right] \tag{12}$$

Dividing Eq. (12) by Eq. (11) element by element, one obtains

$$\mathbf{W}_{m1} = \frac{\mathbf{V}_{\mathrm{D},m1}}{\mathbf{V}_{\mathrm{H},m1}} = \left[1, w_2, \cdots, w_n, w_{n+1}, \cdots, w_{2n}\right] \tag{13}$$

where

$$\begin{cases} w_i = \dfrac{m_i^*}{m_i} \times \dfrac{m_1}{m_1^*} & \left(2 \le i \le n\right) \\ w_i = \dfrac{k_j^*}{k_j} \times \dfrac{m_1}{m_1^*} & \left(n+1 \le i \le 2n,\ j = i-n\right) \end{cases} \tag{14}$$

$\mathbf{W}_{m1}$ is the relative mass and stiffness ratio between the health and damage condition of a structure and can be regarded as a damage detection feature. There are three possible cases for $\mathbf{W}_{m1}$,

(1) No damage occurs: no change happens and all the physical parameters remain constant. In this case, all the components of the damage detection vector $\mathbf{W}_{m1}$ in Eq. (13) equal to 1.

(2) Damage occurs (other structural element parameters may change but m_1): for example when only k_1 decreases, all the components of the vector $\mathbf{W}_{m1}$ will not change and equal to one but w_{n+1}. w_{n+1}, corresponding to k_1, indicates the location of damage. Moreover, w_{n+1}= k_1^*/k_1 shows the magnitude of the damage, i.e., the stiffness change ratio of the 1st element between two conditions.

(3) Damage occurs (m_1 changes): all the components of the vector $\mathbf{W}_{m1}$ change and don't equal to one because of $m_1/m_1^* \neq 1$ in Eq. (14).

In general, structure damage is considered to be caused by few structural element changes relative to the initial condition. Therefore, the solution in case 3 cannot represent the true condition of a structure when the change of all structural elements occurs and is regarded as "abnormal". In this case, the solution fails to indicate structural damage. In order to overcome this problem and to obtain "true solution" and correctly detect damage location and extent, the SEMV $\mathbf{Z}$ in health condition and test condition will both be normalized to all the mass and stiffness parameters m_1~m_n, k_1~k_n one by one. Consequently, the damage detection feature vectors $\mathbf{W}$ can be calculated and formed into a matrix as

$$\mathbf{U} = \left[\mathbf{W}_{m1}, \mathbf{W}_{m2}, \cdots, \mathbf{W}_{mn,} \mathbf{W}_{k1}, \mathbf{W}_{k2}, \cdots, \mathbf{W}_{kn}\right] \tag{15}$$

When an element mass m_i or stiffness k_i changes, only the vector $\mathbf{W}_{mi}$ or $\mathbf{W}_{ki}$ in the damage detection matrix $\mathbf{U}$ will appear as "abnormal". The other vectors in the matrix $\mathbf{U}$, which are normalized to those undamaged structural elements, remain consistent and are termed as "normal solutions". Few of vectors in matrix **U** appear "abnormal" and most vectors in the matrix **U** are "normal" because of the fact that damage is, in many cases, a local phenomenon. In addition, "abnormal solutions" are obviously different and can be easily distinguished from "normal solutions" when they are drawn in one figure.

Consequently, a simple damage detection method based on the SEMV can be established given that actual modal measurements (mode shape $\mathbf{\Phi}$ and frequency f) in health condition and in test condition (mode shape $\mathbf{\Phi}^*$ and frequency f^*) have been provided. The main procedures can be summarized as follows,

(1) Updating model with given measurements. Following the process of section 3.2, a virtual to-be-updated model is established, in which m_1 is chosen randomly (here 1 is chosen only for the convenience of demonstration purpose) and other parameters equal to m_1 consistently ($\hat{m}_i = m_1, \hat{k}_i = m_1$). The corresponding parameters of this model ($\hat{\mathbf{K}}$, $\hat{\mathbf{M}}$, $\hat{\mathbf{K}}_i^e$, $\hat{\mathbf{M}}_i^e$, $\hat{\mathbf{\Phi}}$, $\hat{\lambda}$) are constructed and calculated.

(2) SEMV calculation. Update the given model with modal measurements (mode shape $\mathbf{\Phi}$ and frequency f) according to section two with the CMCM method, and an updated model ($\mathbf{K}$, $\mathbf{M}$, $\mathbf{K}_n^e$, $\mathbf{M}_n^e$, $\mathbf{\Phi}$, f) can be obtained. The correction factors $\boldsymbol{\alpha}$, $\boldsymbol{\beta}$ and the SEMV $\mathbf{V}_{\mathrm{H},m1}$ in Eq. (11) can be calculated and obtained. Likewise, the vector $\mathbf{V}_{\mathrm{D},m1}$ in the test condition can also be calculated.

(3) SEMV normalization. Normalize the SEMV ratio vector $\mathbf{W}_{m1}$ with m_1 as Eq. (13).

(4) Damage detection feature extraction. Assume the mass and stiffness parameters m_1~m_n, k_1~k_n to equal to 1 sequentially and repeat steps (1) ~ (3), and form the damage detection feature matrix **U** in Eq. (15).

(5) Damage identification. All the vectors in the matrix **U** are drawn in one figure in column wise and "abnormal solutions" are eliminated. "Normal solutions" are thus averaged and used to detect damage presence, location and extent.

4. Numerical simulation

In this section, a four-story shear building is studied as a numerical example to demonstrate the detailed procedures of the proposed damage detection method in section three.

4.1 Model description

For a four-story shear building (as shown in Fig. 2), a uniform mass and inter-story stiffness distribution along the height of the building is considered, i.e., $m_1 = m_2 = m_3 = m_4$ $=1.0\times10^5$ kg and $k_1 = k_2 = k_3 = k_4 = 2.04\times10^8$ N/m. The preset damping ratio for each floor is 0.02. Each floor can only move horizontally. In this research, several damage scenarios are designed to investigate the effectiveness of the proposed approach by increasing the story masses or decreasing the inter-story stiffness relative to initial values, as shown in Table 1. State 1 is the baseline of the structure without damage. In state 2, the 1st inter-story stiffness, k_1, has a reduction of 20 percent, which is used to simulate that a single location of damage exists in the building. In state 3, the 1st and 3rd inter-story stiffness are reduced by 20 and 40 percent, respectively, to simulate multiple locations of structural damage. In state 4, the mass of the 2nd floor is increased by 20 percent to simulate that the building is healthy but under operating conditions with appended loading mass. State 5 is for considering that the building is under operational conditions and that multiple damage occurs. This is achieved by a 20 percent mass increase of the 2nd floor and 40 percent reduction of 3rd inter-story stiffness, respectively.

4.2 Modal parameters identification

For this structure, four uncorrelated band-limited white noise, whose bandwidth is from 0 Hz to 50 Hz, were applied to each floor slab to simulate ambient excitations. The maximum of the white noise equal 1. At the same time, four accelerometers are attached to each floor slab to measure the acceleration signals of the building under ambient excitations, as shown in Fig. 2. In this study, the dynamic responses, i.e., accelerations, were simulated from the discrete-time state space model, which was discretized from the continuous state space model of the structure by a zero-order hold (Juang 1994) in which the applied forces are regards to remain constant in each of the sampling periods. The structure was sampled at 3.125 ms intervals corresponding to a sampling frequency of 320 Hz. Each test lasted 25.6s, i.e., 8192 samples were recorded in each test. Fig. 3 presents the applied forces and the measured accelerations in a certain test under baseline condition. The left column shows the applied force on each floor slab, and the right column corresponds to the "measured" acceleration signal of each accelerometer. In practical applications, measured signal is inevitable to be exposed to immeasurable noise contamination. For testing the robustness of the proposed approach, white noise with 5 percent Signal-to-Noise Ratios (SNRs), i.e., SNR = 5%, is mixed into the measured acceleration signals.

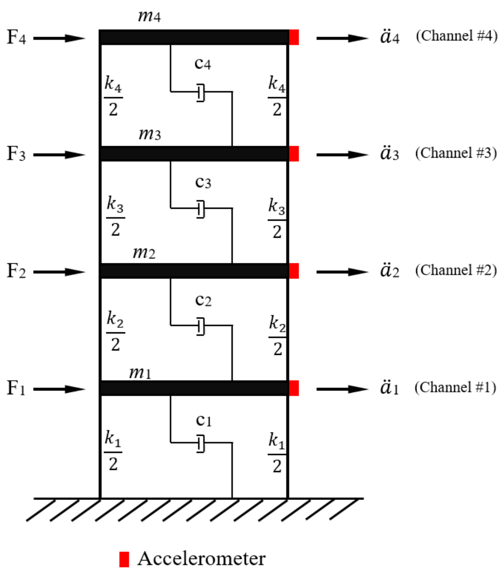

Fig. 2 Model for the numerical simulation

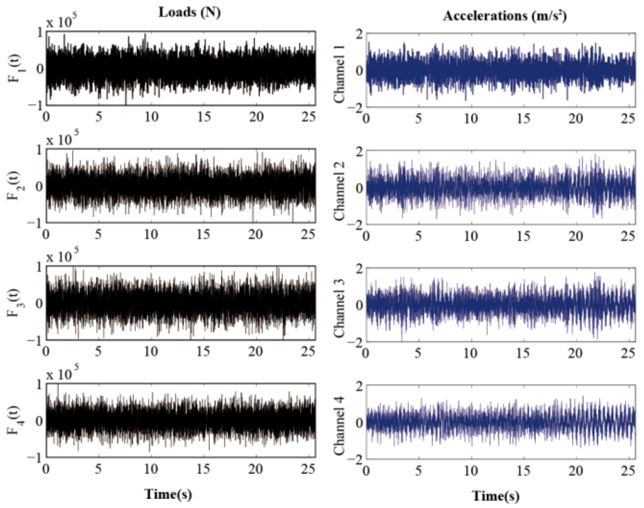

Fig. 3 Loads and measured accelerations in a certain test. Left column: applied ambient force on each floor slab; right column: measured acceleration signal of each accelerometer

Table 1 Summary of structure state conditions

State	Description	State condition
State#1	Baseline	Undamaged
State#2	k1(-20%)	Damaged
State#3	k1(-20%)、k3(-40%)	Damaged
State#4	m2(+20%)	Damaged
State#5	m2(+20%)、k3(-40%)	Damaged

Table 2 Modal parameters of the five states

Conditions	Order	Theoretic frequency (Hz)	LMS modal identification result (SNR = 5%)		
			Frequency (Hz)	Mode shape (MAC)	Damping ratio (%)
State#1	1	2.50	2.48	1.00	0.24
	2	7.19	7.21	1.00	1.11
	3	11.01	11.05	1.00	2.16
State#2	1	2.37	2.37	1.00	2.77
	2	6.93	6.98	1.00	1.89
	3	10.82	10.85	1.00	1.28
State#3	1	2.25	2.26	1.00	0.70
	2	6.24	6.27	1.00	0.99
	3	10.71	10.72	1.00	0.93
State#4	1	2.45	2.43	1.00	1.25
	2	6.96	6.95	1.00	0.65
	3	10.96	10.96	1.00	2.25
State#5	1	2.32	2.33	1.00	0.98
	2	6.25	6.21	1.00	0.98
	3	10.81	10.81	1.00	1.01

After the acceleration signals of each floor were measured, the structural modal parameters (frequency and mode shape) for different test conditions can be identified by various existing modal parameter identification algorithm. In our study, a commercial modal analysis software, LMS test Lab. (Zhang, Jiang *et al.* 2008), was employed here to identify the structural modal parameters. For this software, the core modal parameter identification algorithm is called PloyMax, which is an non-iterative frequency-domain parameters estimation method and presents very good stability, accuracy of the estimated modal parameters and quality of the frequency response function synthesis compared with classical Experimental Modal Analysis (EMA) methods (Petters, Lowet *et al.* 2004a, Petters, Van der Auweraer *et al.* 2014b). Therefore, the modal identification results for five test scenarios in this section can be achieved, as shown in Table 2, in which the modal assurance criterion (MAC) was calculated to evaluate the similarity for the identified mode shape and theoretical mode shape obtained from eigenvalue analysis. Fig. 4 shows the identified mode shapes of the five test conditions for the numerical model. All the identification results demonstrate that the test modal parameters of the structure can be extracted accurately using the LMS test lab. software even under noisy environment (SNR = 5%).

4.3 Damage identification

When all the modal parameters (frequency and mode shape) for the baseline and damage conditions were achieved, according to Eq. (4) in the CMCM method, seven unknown correction factors of the four-story shear building can be calculated and ascertained just from two measured modes, which could derive eight equations. But in practical applications, multiple sets of solutions for the correction factors will appear just based on two measured modes because of the effect of noise. Therefore, the first three mode shapes and corresponding frequencies are adopted to compute the solution in this study, which will enhance the ability of noise robustness and the accuracy of the solution. Fig. 5 shows the solutions. It is easy to distinguish “abnormal solutions” denoted with red from “normal solutions” denoted with blue. The “normal solutions” vectors keep consistent and maintain around the value of 1 at the locations of undamaged elements, however, large fluctuation appears near the location of damaged elements. Fig. 6 shows the average values of “normal solutions” after eliminating “abnormal solutions”, and presents more obvious damage identification results than Fig. 5. The location and extent of damage is accurately demonstrated in Fig. 6.

To evaluate the effect of noise contamination to the proposed method, the noise level is then increased from 5 percent to 10 percent and damage detection result is shown in Figs. 7 and 8. The vectors in the SEMV solution matrix **U** does not appear more obviously dispersed under the 10 percent noise level in Fig. 7, and “normal solutions” can still be clearly distinguished from “abnormal solutions”. The damage identification result is consistent with that of the 5 percent noise level. To further examine the effects of noise, 20 percent noise is added in the mode shapes. In this case, the damage element can still be located although the solution matrix **U** is much more dispersed. However, it becomes difficult to evaluate the damage extent because “abnormal solutions” and “normal solutions” have been mixed and could not be easily separated from each other. As space is limited, the detection result will not be listed.

All the detection results demonstrate that the consistency of normal solutions decreases and relative structural changes tend to be overwhelmed with the increase of SNRs. However, the identified results are still reliable, even when a 10 percent proportional white noise is being mixed. The strong robust ability of the proposed method may be attributed to the outstanding advantage of the CMCM model updating algorithm employed in this numerical study, three measured modes were attended to the calculative procedure and could provide twelve equations, which was considered enough to solute the seven unknown correction factors, the remaining solution equations could enhance the ability of noise robustness and the accuracy of the solution.

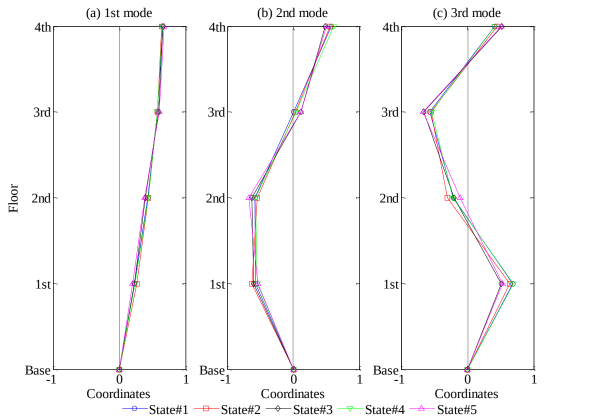

Fig. 4 Identified mode shapes for five test conditions of the numerical model

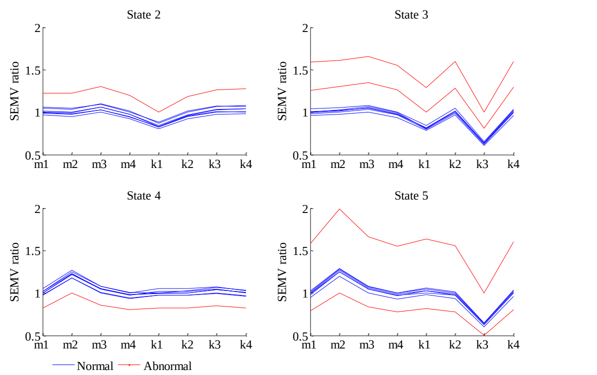

Fig. 5 SEMV solution matrix **U** for four damage states under noisy environment (SNR = 5%)

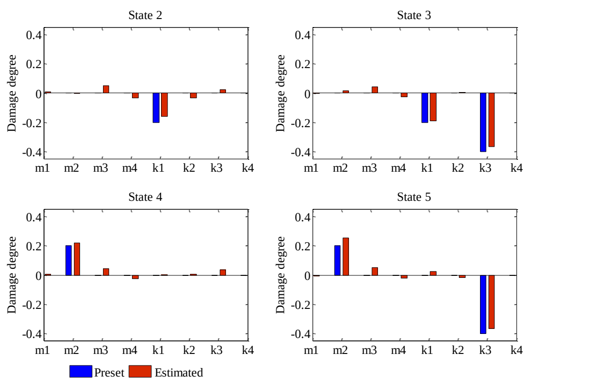

Fig. 6 Damage detection for four states under noisy environment (SNR = 5%)

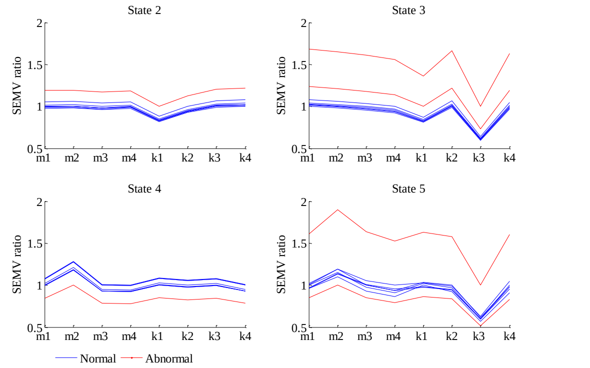

Fig. 7 SEMV solution matrix **U** for four damage states under noisy environment (SNR = 10%)

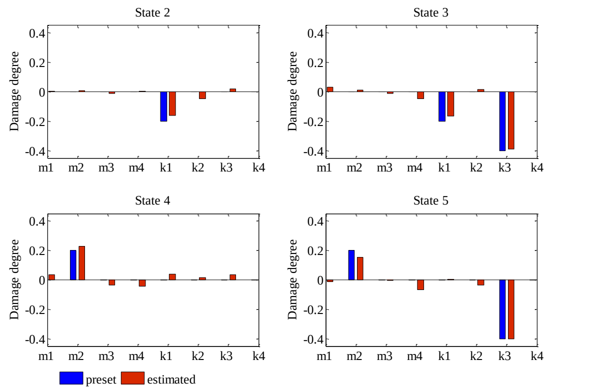

Fig. 8 Damage detection result for four states under noisy environment (SNR = 10%)

5. Lanl test-bed structure

In this section, experimental tests at the Los Alamos National Laboratory (LANL) are used to validate the damage detection ability and to illustrate the application of the proposed method.

5.1 Model description

The LANL three-story shear-building is shown in Fig. 9. It consists of four aluminum plates (30.5×30.5×2.5 cm) connected by bolted joints to four aluminum columns (17.7×2.5×0.6 cm) at each floor (Figueiredo, Park *et al.* 2009). An additional element (15×2.5×2.5 cm) attached to the top floor and an adjustable bumper mounted on the second floor can be used to introduce a gap nonlinearity in the system. The gap distance can be modified by adjusting the position of the bumper to vary the level of the nonlinearity. The whole structure is mounted on two rails to allow the system to slide only in one direction. An electro-dynamic shaker was used to provide a band-limited random base excitation (20-150 Hz) to the test structure.

The deployed sensor network consists of four accelerometers and a force transducer with nominal sensitivities of 1000 mV/g and 2.2 mV/N, respectively. The accelerometers were attached to each aluminum plate along a vertical center line to measure the dynamic response of the 4DOF lab structure. The force transducer was connected to the tip of the stinger to gauge the input force generated by the shaker. The sensor's measurements were recorded at a sampling frequency of 322.58 Hz by a data acquisition system. Full details concerning the LANL test setup are documented in (Figueiredo, Park *et al.* 2009).

The structural changes in the system were physically simulated through variations in either the mass or stiffness of the reference structure. The mass of the system was modified by attaching a 1.2 kg concentrated mass (approximately 19.1% of the total mass of each floor) to the aluminum plates. The changes in stiffness were introduced by reducing one or more columns' stiffness by 87.5%. This process was done by replacing the corresponded column with another one with half the cross-section thickness in the direction of shaking. The five structural state configurations considered in this study are summarized in Table 3.

Table 3 Summary of structural state conditions

Label	Condition	Description
State#1	Reference condition	——
State#2	19.1% 1st-story mass increment	1.2kg additional mass on the 1st-story
State#3	21.8% 1st-story stiffness reduction	Exchange one columns on the 1st-story
State#4	21.8% 3rd-story stiffness reduction	Exchange one columns on the 3rd-story
State#5	43.7% 3rd-story stiffness reduction	Exchange two columns on the 3rd-story

Table 4 Identified mode frequencies and damping ratios of five states

	Order	State# 1	State# 2	State# 3	State# 4	State# 5
Frequency (Hz)	1	30.92	30.98	30.39	29.74	28.67
	2	54.80	53.78	51.61	51.41	47.56
	3	71.64	69.15	70.06	70.10	69.24
Damping (%)	1	2.92	2.56	2.83	2.47	2.56
	2	0.74	1.41	0.79	0.86	1.11
	3	0.55	0.44	0.31	0.42	0.40

Fig. 9 LANL-4 DOF test-bed structure experiment

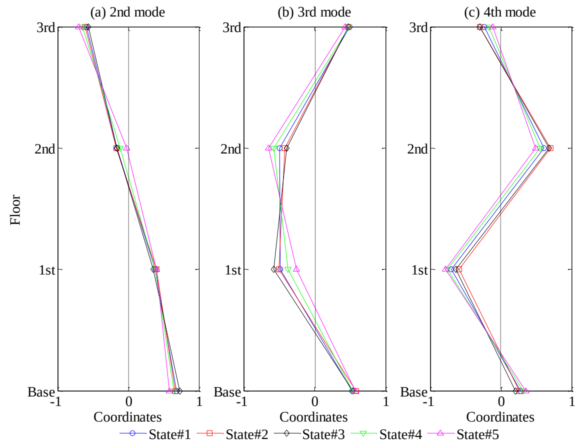

Fig. 10 Experimental mode shape for five test conditions

Although the test-bed structure had an adjustable nonlinear gap in the third floor, it was set to keep the system within the linear range during the dynamic tests conducted in this study. The modal frequencies and damping of five structural states identified using ERA algorithm (Juang 1994) are summarized in Table 4. Fig. 10 shows the identified mode shapes for the five test states. It should be noted that only the lower three mode shapes and frequencies from the experimental study are used.

5.2 Damage identification result

The identification results of the four damage states using the proposed method are shown in Figs. 11 and 12. For the LANL experiments, the "abnormal solutions" in the SEMV solution matrix **U** corresponding to four damage conditions can be distinguished from "normal solutions" conveniently, as shown in Fig. 11. The "normal solutions" keep consistent and clearly show the location of damage, where the "normal solutions" have valleys. After eliminating "abnormal solutions", the average values of the "normal solutions" can locate and quantify structural damage more obviously and accurately as shown in Fig. 12. Thus, the ability of the proposed approach for damage identification is convincingly verified by the LANL experiments.

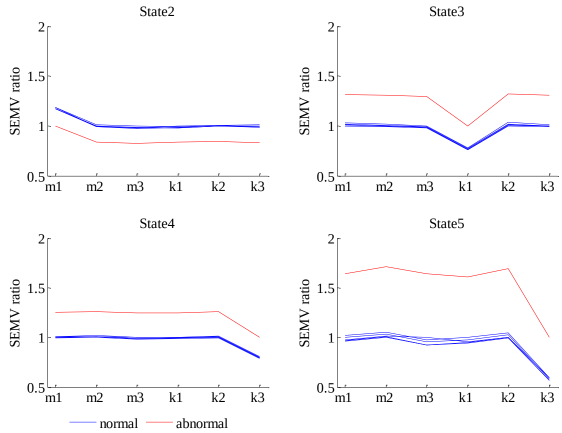

Fig. 11 SEMV solution matrix **U** in four damage states

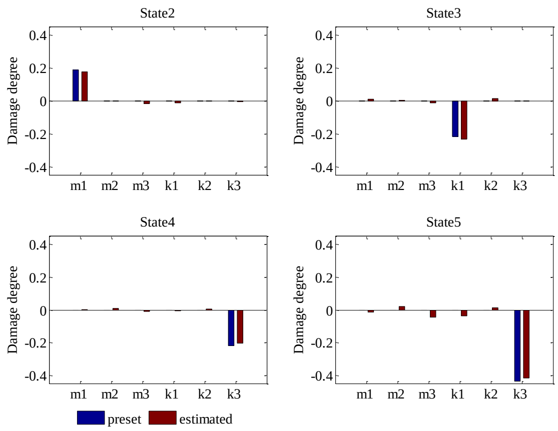

Fig. 12 Damage identification result in four damage conditions

6. Conclusions

A new damage detection approach is proposed based on the structural element mass-stiffness vector (SEMV). First, a virtual model is assumed and then updated with the CMCM method. The SEMV ratio is then extracted as a damage detection feature by comparing the SEMV in health condition with damage condition, and finally the "normal solutions" of the SEMV ratio solution matrix **U** are averaged after eliminating "abnormal solutions". The averaged SEMV ratio "normal solutions" show the location and extent of structural damage.

The proposed approach has been validated by a numerical simulation example and the LANL experiments of a three-story structure. Both the results demonstrate that the proposed approach is able to detect the presence of structural change, locate the structural section where the change occurred, and provide an accurate estimation of actual level of "changes". The proposed method coalesces two kinds of damage identification methods based on model and measured data, and takes full advantages of both kinds of methods: (1) no physical parameters (the element mass and stiffness) of actual structure are needed but the measured acceleration signals in health and damage conditions; (2) not only structural element stiffness decrease but also element mass change can be identified. (3) both damage location and extent can be accurately detected and evaluated.

Acknowledgements

The authors are indebted to Professor Sami F. Masri for the introduction of the chain-like method. Furthermore, this work was partially supported by the Major State Basic Research Development Program of China (973 Program, grant number 2015CB057704), National Natural Science Foundation of China (Grant number 51121005 and 51578107), and Chinese Scholarship Council (CSC). The authors would like to thank for them for their financial support.

References

Carden, E.P., and Fanning, P. (2004), "Vibration based condition monitoring: a review", *Struct. Health Monit.*, **3**(4), 355-377.

Doebling, S.W., Farrar, C.R.. and Prime, M.B. (1998), "A summary review of vibration-based damage identification methods", *Shock Vib. Digest*, **30**(2), 91-105.

Fan, W. and Qiao, P. (2011), "Vibration-based damage identification methods: a review and comparative study", *Struct. Health Monit.*, **10**(1), 83-111.

Farrar, C.R., and Worden, K. (2012), *Structural health monitoring: A machine learning perspective*, John Wiley & Sons, Chichester, West Sussex, U.K.

Figueiredo, E., Park, G., Figueiras, J., Farrar, C. and Worden, K. (2009), "Structural health monitoring algorithm comparisons using standard data sets", Research Report No. LA-14393; Los Alamos National Laboratory (LANL), Los Alamos, NM (United States).

Hernandez-Garcia, M.R., Masri, S.F., Ghanem, R., Figueiredo, E. and Farrar, C.R. (2010), "An experimental investigation of change detection in uncertain chain-like systems", *J. Sound Vib.*, **329**(12), 2395-2409.

Hu, S.L.J., Li, H. and Wang, S. (2007), "Cross-model cross-mode method for model updating", *Mech. Syst. Signal Pr.*, **21**(4), 1690-1703.

Juang, J.N. (1994), *Applied system identification*, Prentice Hall, Englewood Cliffs, New Jersey, USA

Li, H.N., Li, D.S. and Song, G.B. (2004), "Recent applications of fiber optic sensors to health monitoring in civil engineering", *Eng. Struct.*, **26**(11), 1647-1657.

Masri, S., Bekey, G., Sassi, H. and Caughey, T. (1982), "Non-parametric identification of a class of nonlinear multidegree dynamic systems", *Earthq. Eng. Struct. D.*, **10**(1), 1-30.

Pandey, A., Biswas, M. and Samman, M. (1991), "Damage detection from changes in curvature mode shapes", *J. Sound Vib.*, **145**(2), 321-332.

Peeters, B., Lowet, G., Van der Auweraer, H. and Leuridan, J. (2004), "A new procedure for modal parameter estimation", *J. Sound Vib.*, **38**(1), 24-29.

Peeters, B., Van der Auweraer, H., Guillaume, P. and Leuridan, J. (2004), "The PolyMAX frequency-domain method: a new standard for modal parameter estimation", *J. Shock Vib.*, **11**(3-4), 395-409.

Roy, K. and Ray-Chaudhuri, S. (2013), "Fundamental mode shape and its derivatives in structural damage localization", *J. Sound Vib.*, **332**(21), 5584-5593.

Sampaio, R., Maia, N. and Silva, J. (1999), "Damage detection using the frequency-response-function curvature method", *J. Sound Vib.*, **226**(5), 1029-1042.

Sohn, H., Farrar, C.R., Hemez, F.M., Shunk, D.D., Stinemates, D.W., Nadler, B.R. and Czarnecki, J.J. (2004), *A review of structural health monitoring literature: 1996-2001*: Los Alamos National Laboratory Los Alamos, NM.

Tomaszewska, A. (2010), "Influence of statistical errors on damage detection based on structural flexibility and mode shape curvature", *Comput. Struct.*, **88**(3), 154-164.

Wang, J. (2009), "Study on damage detection and model updating for offshore platform structures", Ph.D, Dissertation, Ocean University of China, Qingdao. (in Chinese)

Worden, K. and Tomlinson, G. (1989), "Application of the restoring force surface method to nonlinear elements", *Processings of the 7th International Modal Analysis Conference*, Las Vegas, NV.

Zhang, C. and Song, G.Q. (2012), "Bridge damage identification by finite element model updating with Tikhonov regularization and wavelet denoising", *J. Vib. Eng*., **25**(1), 98-102.

Zhang, L., Jiang, F., Wang, Y. and Zhang, X. (2008), "Measurement and analysis of vibration of small agriculturalmachinery based on LMS Test. Lab", *Transactions of the Chinese Society of Agricultural Engineering*, **24**(5),100-104.

Zhu, H., Li, L. and He, X.Q. (2011), "Damage detection method for shear buildings using the changes in the first mode shape slopes", *Comput. Struct*., **89**(9), 733-743.

BS